Journal of the European Ceramic Society 36 (2016) 3249–3256

Contents lists available at www.sciencedirect.com

Journal of the European Ceramic Society

journal homepage: www.elsevier.com/locate/jeurceramsoc

Additive manufacturing of boron carbide via continuous filament direct ink writing of aqueous ceramic suspensions

William J. Costakis Jr.*, Lisa M. Rueschhoff, Andres I. Diaz-Cano, Jeffrey P. Youngblood, Rodney W. Trice

School of Materials Engineering, Purdue University, West Lafayette, IN 47907, USA

ARTICLE INFO

Article history:
Received 4 March 2016
Received in revised form 31 May 2016
Accepted 1 June 2016
Available online 15 June 2016

Keywords:
Boron carbide
Additive manufacturing
Direct ink writing
Aqueous ceramic processing
Rheology

ABSTRACT

Direct ink writing, a type of additive manufacturing, has been used to fabricate near-net shaped boron carbide (B_4C) specimens at room temperature with aqueous suspensions. Suspensions with B_4C solids loading of 48–56 vol.% were dispersed with polyethlenimine (PEI, 25,000 and 750,000 g/mol) and exhibited yield-pseudoplastic behavior. Specimens with filament layer shape retention were produced with suspensions with 50–56 vol.% B_4C and yield stresses ≥43 Pa and equilibrium storage moduli ≥700 Pa. No residual porosity or cracking between deposited layers was observed in any samples. However, warpage was observed in some green body specimens and was minimized through use of a low molecular weight polymer and reduction of the B_4C solids loading. Optimal specimens with high filament layer shape retention and no warpage were produced with suspensions containing 54 vol.% B_4C and 25k g/mol PEI.

1. Introduction

Boron carbide (B_4C) possesses a low density (2.52 g/cm^3), a high melting point (~2450 °C), low chemical reactivity, and high hardness, making it an ideal material for extreme environment applications [1,2]. Common applications for B_4C include: high wear components, control rods for fast-breeder nuclear reactors, and light-weight armor applications [1]. To achieve these favorable properties, however, B_4C must be sintered to full density. B_4C has historically been sintered using externally applied pressure, via hot pressing or hot isostatic pressing, due to the challenges associated with densification [2–5]. Hot pressing limits the geometries of the final pieces to simple shapes such as pellets, plates, disks, and rods [6]. Hot isostatic pressing (HIP), on the other hand, allows for the sintering of more complex shapes formed through processes such as slip, tape, or gel casting [7,8]. However, it must also be noted that there are limitations associated with these types of forming processes when used with B_4C and other ceramics [9]. Slip and tape casting have the ability to form cost effective near-net shapes but are limited to simple structures and require complex secondary machining to add intricate features [7,10]. While, gel casting has the ability to produce complex-shaped parts it typically requires suspensions with harsh crosslinking polymers or curing agents, and is limited by the complexity of the mold [7,9]. Ultimately, there is a need to develop forming methods that will allow for the cost-effective production of near-net and complex-shaped parts of B_4C.

Additive manufacturing techniques are rapidly gaining interest among the academic and industrial communities due to the ability to form complex shapes of materials that are difficult to cast or machine [11–15]. Direct ink writing is a form of additive manufacturing that uses a computer controlled system to deposited ceramic inks in a controlled fashion. This forming process can be divided into two main categories: droplet or filament based [14,16]. Droplet-based direct ink writing techniques deposit formed droplets of the binding material in a desired pattern to generate a layer-by-layer configuration [16]. Filament direct ink writing is an extrusion-based additive manufacturing process that deposits aqueous colloidal suspensions of ceramic powders in a continuous layer-by-layer fashion to produce complex-shaped dense ceramic parts [15,16]. Inks used in filament direct writing processes are typically composed of ceramic powders, a water-soluble polymer dispersant, and water and do not require crosslinking polymer or curing agents [14–17]. The rheological properties of the suspensions are designed to have a yield stress. Once the applied shear stress exceeds the yield stress, the suspension flows and parts can be constructed by rastering the extrudate

* Corresponding author.
E-mail address: rtrice@purdue.edu (W.J. Costakis Jr.).

http://dx.doi.org/10.1016/j.jeurceramsoc.2016.06.002
0955-2219/

in a controlled fashion, building up the part layer by layer. Upon removal of the shear stress the yield stress of the suspension quickly develops again, prohibiting the formed part from slumping due to either gravity or its own weight [9,15,17–19]. Suspensions are typically designed with high solids loading for two reasons. First, increased powder loading tends to increase the yield stress of the suspension, necessary for building parts with multiple stacked layers to avoid slumping. Second, increasing the powders loading increases the green body density, thus there is less porosity to remove during sintering [6,16,17].

Using continuous filament direct ink writing as an additive manufacturing technique has allowed the production of complex-shaped parts of many different ceramic systems including mullite, alumina, stabilized zirconia, and silicon nitride at solids loading greater than 50 vol.% [12,15,16,19,20]. Even with this strong interest to form complex ceramic structures, there has yet to be any significant development with producing B_4C shapes through the use of additive manufacturing primarily due to problems associated with forming aqueous suspensions with high solids loading. To continuously direct write B_4C, stable aqueous ceramic suspensions with the desired rheological properties have to be developed.

Previous research on aqueous colloidal processing of B_4C has been limited to slip and tape casting processes [6,7,10,21,22]. Leo et al. [6] reported that aqueous slip casting slurries of B_4C were only stable up to 40 vol.% when using 2.6 μm powders and Darvan C-N, an ammonium salt of poly(methacrylic acid) (PMAA), as a dispersant. As stated previously, higher solids loading must be used in a direct writing approach to achieve the desired rheological properties and higher green body packing densities [6,17]. Furthermore, other studies have reported that suspensions with higher solids loading minimize drying-induced crack formation and phase segregation while promoting higher sintered densities [6,12,17]. It is possible that the low molecular weight of Darvan C-N (10,000–16,000 g/mol) used by Leo et al. [6], was not enough to stabilize the B_4C particles, as larger molecular weight polymers have been shown in previous studies to offer higher dispersion via steric stabilization [20,23]. Higher solids loadings (>50 vol.%) of B_4C were achieved by Li et al. [10], but were only possible using acid-treated powders dispersed with tetramethylammonium hydroxide (TMAH) an ammonium salt and a mixture of water-borne epoxy emulsions and urethanes emulsions as the green body binder [7,10]. The suspensions formed in the study performed by Li et al. [10], are suitable for gel and tape casting but would lack the required viscoelastic properties as well as the drying dynamics that are required of direct ink writing. Therefore, it is necessary to develop highly loaded aqueous B_4C suspensions dispersed with a high molecular weight polymer while having the desired viscoelastic and rheological properties to facilitate the direct ink writing process.

The present study aims to produce near-net shaped B_4C green-bodies using direct ink writing of highly loaded aqueous suspensions. Our approach to fabricate suspensions with maximum solids loading and ideal yield stresses and viscoelastic properties for direct writing, was to use a cationic polyelectrolyte dispersant (polyethlenimine or PEI) with a high molecular weight to afford greater particle stability via steric repulsion. PEI was chosen due to its large electrostatic potential with B_4C [24], as previous research has shown that a high electrostatic potential will allow for the stabilization of ceramic powders and suspensions with desirable flow properties [25]. The suspensions formulated for the current study are a mixture of 48–56 vol.% B_4C, 5 vol.% (PEI) polymer dispersant, 5 vol.% hydrochloric acid (HCl), and a balance of water. This study will assess the effects of PEI molecular weight and B_4C solids loading on the rheology and quality of final specimens produced via direct ink writing.

2. Experimental procedures

2.1. Boron carbide suspension preparation

One hundred grams of grade HS boron carbide (H.C. Starck, Germany) were suspended in 150 mL of 200 proof ethanol and were attrition milled at 50 RPM with 1 kg of 3.2 mm diameter WC milling media (Union Process, Akron, OH) for 2 h [26,27]. After attrition milling, the ethanol was evaporated at 150 °C for 24 h. The mass of the milling media was weighed before and after attrition milling to evaluate the amount of WC that was introduced into the system. Each batch of attrition milled powders had roughly 2.7 vol.% residual WC. A Beckman Coulter LS 230 particle size analyzer (Brea, CA) was used to determine the average B_4C particle size before and after attrition milling. A particle size of 3.73 ± 1.27 μm and 1.72 ± 0.35 μm was obtained for pre- and post-attrition milled B_4C powders, respectively with the residual WC having an average particle size of 0.15 ± 0.06 μm.

Preliminary zeta potential analysis [24] using a ZetaSizer Nano Z (Malvern Instruments Ltd, Worcestershire, UK) revealed that attrition milled B_4C in a polyethylenimine (PEI, Sigma–Aldrich, St. Louis, MO) and reverse osmosis (RO) water solution had a maximum potential of ±70 mV at a wide pH range (5–8). The pH of the suspensions was lowered with 5 vol.% hydrochloric acid (37% HCl, Sigma–Aldrich, St. Louis, MO) solution in order to achieve suspensions in the optimum range as it is considered that zeta potential values greater than 30 mV afford moderate colloidal stability [28]. The pH of the final suspensions was measured using an Oakton pH 5 m (Vernon Hills, IL), which was calibrated with electrolytic buffer solutions of pH 4 and 10. The pH values of the final suspensions were all in the range of 5.35–5.91. PEI average molecular weights of 25,000 (25k) g/mol and 750,000 (750k) g/mol were used in this study. The large molecular weight of either PEI molecules allows it to act both as an electrosteric dispersant and green body binder.

Attrition milled B_4C powders were incrementally added to the PEI and (RO) water solution in a 250 mL Nalgene bottle to produce highly-loaded aqueous suspensions. These suspensions were mixed with four 12.7 mm diameter WC milling media (Union Process, Akron, OH) in a Dual Asymmetric Centrifuge (DAC 450, Flacktek, Landrum, SC). Powders were mixed at 800 RPM for 60 s and 1200 RPM for 60 s until all the B_4C was added and sufficiently dispersed. The suspensions were then ball milled for 24 h to achieve complete uniformity. The B_4C solids loading and water content were systematically altered to determine the optimal rheological properties for forming and are shown in Table 1. All suspensions had nominally 5 vol.% PEI and 5 vol.% HCl added.

2.2. Rheological characterization

The rheological and viscoelastic properties of the B_4C suspensions were measured using a Malvern Bohlin Gemini HR rheometer (Malvern Instruments Ltd., Worcestershire, UK) with a 25 mm cup and bob geometry fixture with a gap of 150 μm. Roughly 13 mL of the suspension was used in each analysis. To minimize premature evaporation of the suspension, a water trap was attached to the system during the test.

Flow curves were obtained for each suspension by measuring the shear response for controlled shear rates increased logarithmically from 0.01 to 35 s^{-1}. Each curve was fitted to the Herschel-Bulkley model for yield-pseudoplastic materials [29], displayed in the following equation:

$$\sigma = \sigma_y + k\dot{\gamma}^n$$

where σ is the shear stress, σ_y is the yield stress for the material, k is the consistency index, $\dot{\gamma}$ is the applied shear rate on the suspension,

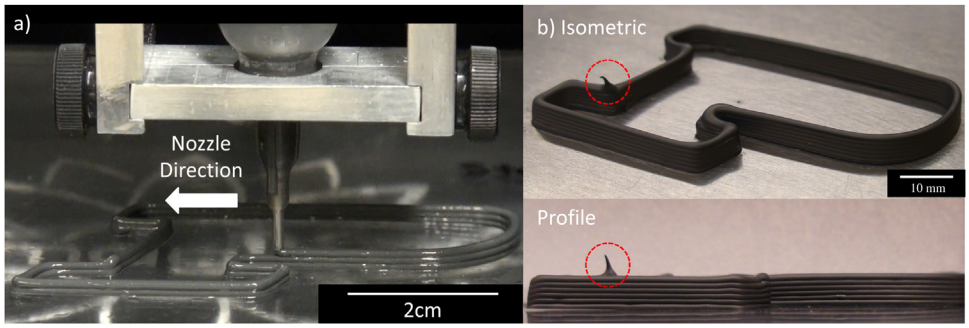

Fig. 1. (a) Image of a B_4C suspension being extruded in a layer-by-layer fashion to form the Purdue "P" shape. (b) Isometric and profile image of a Purdue "P" specimen produced via direct ink writing a 54 vol.% B_4C suspension. A dashed circle indicates the starting (and stopping point) for each layer.

Table 1
Compositions of B_4C suspensions with corresponding Herchel-Bulkley curve fitting parameters for yield-pseudoplastic fluids. The equilibrium storage modulus is provided. Warpage displacement (X) is the measurement from a flat surface to the bottom of the B_4C green body specimen at the maximum point of displacement. Average layer height is the averaged cross sectional height (Y) of individual green body filament layers. The optimum suspension is shown in bold. An (*) denotes samples with estimated Herchel-Bulkley fit parameters due to low statistical measurements ($R^2 < 0.95$).

PEI Molecular Weight [g/mol]	B_4C [vol.%]	Water [vol.%]	σ_y [Pa]	k [Pa s^n]	n	G'_{eq} [Pa]	Warpage Displacement [mm]	Average Layer Height [mm]
25,000	50	40	24	11.6	0.44	64	0.0	–
25,000	52	38	37	22.3	0.46	274	0.0	–
25,000	**54**	**36**	**122**	**51.3**	**0.46**	**962**	**0.0**	**0.79 ± 0.07**
25,000	56	34	359*	66.5*	0.47*	3418	0.8	0.85 ± 0.05
750,000	48	42	20	14.6	0.38	155	0.0	–
750,000	50	40	43	15.3	0.42	767	1.25	0.67 ± 0.12
750,000	52	38	83	55.4	0.36	1844	2.75	0.73 ± 0.08
750,000	54	36	352*	108.9*	0.25*	3760	4.50	0.76 ± 0.04

and n is the flow index. The flow index is a measurement of the degree of shear rate dependence of a fluid, and shear-thinning fluids will have an index number of less than 1 [30]. A simple regression analysis was used to calculate the yield stress and flow index of each suspension.

A stress sweep analysis was performed for each suspension by measuring the storage shear modulus (G') for an applied oscillation stress ranging from 1 to 1000 Pa at a frequency of 1 Hz. A pre-shear of 30 s^{-1} was applied for 30 s followed by an equilibrium time of 100 s.

2.3. Direct writing process

A commercially available syringe style printer with layer-by-layer deposition capabilities was used to direct write specimens. Previous studies optimized the use of a modified Imagine 3D printer (Essential Dynamics, New York City, NY), which was employed in this study [19]. An EFD (Nordson EFD, East Providence, RI) 10 mL syringe with a tip capillary length of 6.5 mm and internal exit radius of 0.625 mm was used. A motor with a gear ratio of 231:1 (Snap Motors, Berkeley, CA) was used to mechanically drive a plunger into the syringe and extrude the suspension. The plunger is programmed to move at a set deposition rate (0.007 mm/s) as shown in Table 2. Fig. 1a shows a B_4C suspension being extruded in a layer-by-layer fashion into a Purdue University "P" shape to demonstrate the capability of forming multiple radii, angles, and straight path functions. An image of the test shape is shown in Fig. 1b. The syringe holder was suspended by a gantry crane system that consists of multiple belts, gear pulleys and motors used to translate the printer head along the respective X-and Y-axes. A build platform was translated along the Z-axis to facilitate the stacking of multiple layers.

FabStudio and FabInterpreter software (Fab@Home project) was used to communicate between the printer and the computer. The software used an algorithm to create a path file for the printer to follow based on a 3D CAD file. Predetermined processing parameters, displayed in Table 2, are built into each file that is generated and were held constant for all specimens.

Table 2
Parameters used to direct write aqueous B_4C suspensions.

Parameter	Value	Description
Slice Height	0.85 mm	deposited layer height
Path Speed	4 mm/s	speed of syringe nozzle
Path Width	1 mm	deposited layer width
Deposition Rate	0.007 mm/s	extrusion rate of suspension
Pushout	0.05 s	time of plunger forward motion prior to the start of each layer
Suckback	0.05 s	time of plunger backward motion at the end of each layer
Suckback Delay	0 s	delay time between end of layer and suckback
Clearance	2 mm	height of syringe nozzle above the previously deposited layer

2.4. Binder burn-out and pressureless sintering

Preliminary thermogravimetric analysis (TGA, TA Instruments, Newcastle, DE) on PEI burn-out in a flowing argon environment indicated a significant weight loss between the temperatures of 300 °C and 450 °C [24]. Based on the TGA results, binder burnout was carried out in a flowing argon environment with a ramp rate of 4 °C/min to 425 °C, followed by 1.5 °C/min to 500 °C, where it was isothermally held for 25 h. Specimens were cooled to room temperature using a cooling rate of 10 °C/min. Sintering was carried out without an external applied pressure in a high-temperature argon environment furnace (Centorr Vacuum Industries, Nashua, NH). The furnace was quickly ramped from room temperature to 300 °C, followed by a heating rate of 25 °C/min to 2000 °C where it was held isothermally for 1 h, followed by rapid cooling to room temperature.

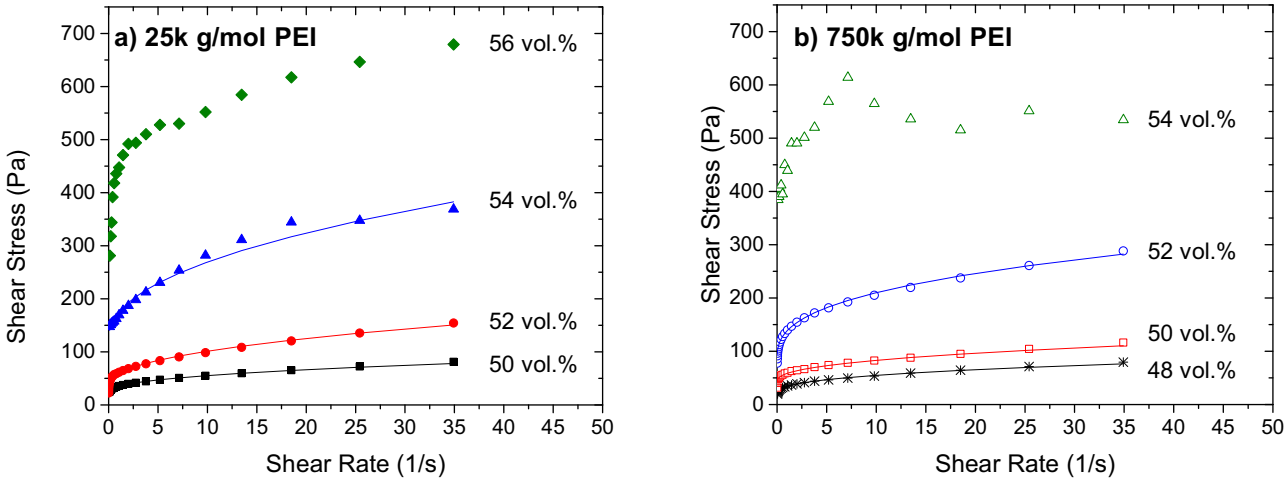

Fig. 2. Flow curves of varying B_4C suspensions with (a) 25k g/mol and (b) 750k g/mol PEI molecular weight. Solid lines correspond to a fit of the Herschel-Bulkley fluid model with fitting parameters ($R^2 > 0.98$) for each data set shown in Table 1. An increase in solids loading and polymer molecular weight both led to higher yield stresses.

2.5. Microstructures and densities

Sintered samples were prepared for microstructural analysis by surface grinding with 200, 400, and 800 grit diamond discs, followed by polishing with 6 μm and 3 μm diamond paste and a 0.06 μm colloidal silica suspension. The microstructure of sintered specimens was analyzed with a Phenom ProX desktop (Phenom-World, Eindhoven, Netherlands) scanning electron microscope (SEM).

To verify the amount of residual tungsten carbide from the attrition milling process, chemical analysis of sintered specimens was performed by NSL Analytical Services, Inc. (Cleveland, OH) using inductively coupled plasma optical emission spectrometry (ICP-OES). The oxygen content of sintered samples was analyzed by the Leco Furnace method. Prior research investigating aqueous processing of zirconium diboride has shown that the oxygen content is correlated with the amount of boria (B_2O_3) [28].

The average bulk density of sintered samples was determined via Archimedes' method in accordance with ASTM C 37314 [31]. The residual WC acquired from attrition milling was accounted for when calculating the true, pore free density of the sintered pieces. The values used in these calculations for B_4C and WC were 2.52 g/cm^3 and 15.63 g/cm^3, respectively. A true density of 2.88 g/cm^3 was calculated for a dense B_4C body with 2.7 vol.% WC.

3. Results and discussion

3.1. Rheological and viscoelastic characterization of suspensions

Flow curves demonstrating the dependence of shear stress on applied shear rate for the B_4C suspensions are shown in Fig. 2 for PEI molecular weights of (a) 25k g/mol and (b) 750k g/mol. These flow curves reveal that all suspensions behaved in a yield-pseudoplastic manner with flow index (n) values of less than 1 indicating a shear-thinning behavior. Yield-pseudoplastic suspensions are ideal for continuous direct writing as they will flow in a shear thinning manner after an applied shear stress exceeds the yield stress and retain the formed shape while supporting other deposited layers after extrusion [15–17,32]. The solid lines correspond to a fit of the Herschel-Bulkley fluid model, with fitting parameters listed in Table 1. The fit of all suspensions, as determined by the R^2 value, was >0.98. The measured pH values for all suspensions were in the range of 5.35–5.91. This small difference in pH values between the suspensions is unlikely to impact the rheological behavior of the suspensions as the zeta potential values over this pH range is relatively constant and approximately ±70 mV [24].

It was found that an increase in the B_4C solids loading and PEI molecular weight led to an increase in the yield stress (σ_y). Different studies with alumina and alumina-zirconia mixed suspensions showed that an increase in solids loading decreased the mean inter-particle spacing leading to a reduction in the interaction volume between the particles and an increase in the yield stress [28,33]. An increase in polymer molecular weight has also been shown to increase suspension yield stress through both chain entanglements and bridging between ceramic particles [9,34,35].

All suspensions, except for the 56 vol.% B_4C suspension with 25k g/mol PEI and 54 vol.% B_4C suspension with 750k g/mol PEI, behaved in a uniform yield-pseudoplastic manner. These particular suspensions did not display the uniform shear-thinning behavior after their characteristic yield stress. Rheological data for these suspensions were considered unreliable due to wall slip between the suspension and the surface of the rheometer cup. A study focusing on the rheology of zirconia suspensions dispersed in a nonpolar organic medium found that highly flocculated system will experience this wall slip phenomenon due to low rheometer wall surface roughness and large flocs in the suspension [36]. Therefore, increasing the surface roughness of the rheometer walls may alleviate this observed effect.

Fig. 3a and b shows the viscosity versus shear rate relationships for the suspensions as a function of PEI molecular weight. All suspensions behaved in a uniform shear-thinning manner within the forming range. An increase in viscosity or consistency index (k) was observed for increasing B_4C solids loading and polymer molecular weight. An increase in the solids loading has been shown to increase the viscosities of ceramic suspensions due to an increase in the inter-particle interactions and inter-particle collisions [15,32,37,38]. A study with aqueous alumina suspensions dispersed with polyvinylpyrrolidone showed that an increase in polymer molecular weight increased the viscosity of the suspensions due to the increase in chain entanglements [18,34,35].

Plots of storage shear modulus versus oscillation stress for the B_4C suspensions as a function of PEI molecular weight are shown in Fig. 4a (25k g/mol) and b (750 kg/mol). Each suspension displayed an equilibrium modulus (G'_{eq}) within the linear viscoelastic region. Values for each suspension are reported in Table 1. It was found that an increase in the B_4C solids loading and/or PEI molecular weight led to an increase in the equilibrium modulus, indicating an increase in gel strength. It has been shown that direct-writing

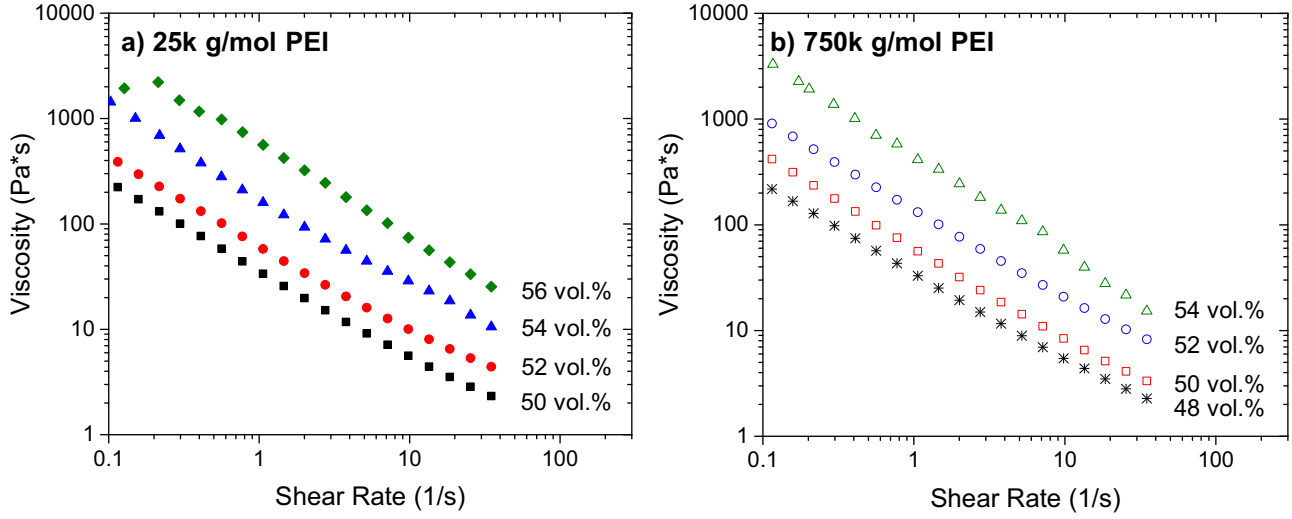

Fig. 3. Log viscosity vs log shear rate plots of varying B_4C suspensions with (a) 25k g/mol PEI and (b) 750k g/mol PEI molecular weight. Increasing the B_4C solid loading resulted in an increase in viscosity for respective molecular weight PEI. Viscosity data illustrates the uniform shear thinning behavior of all the suspensions.

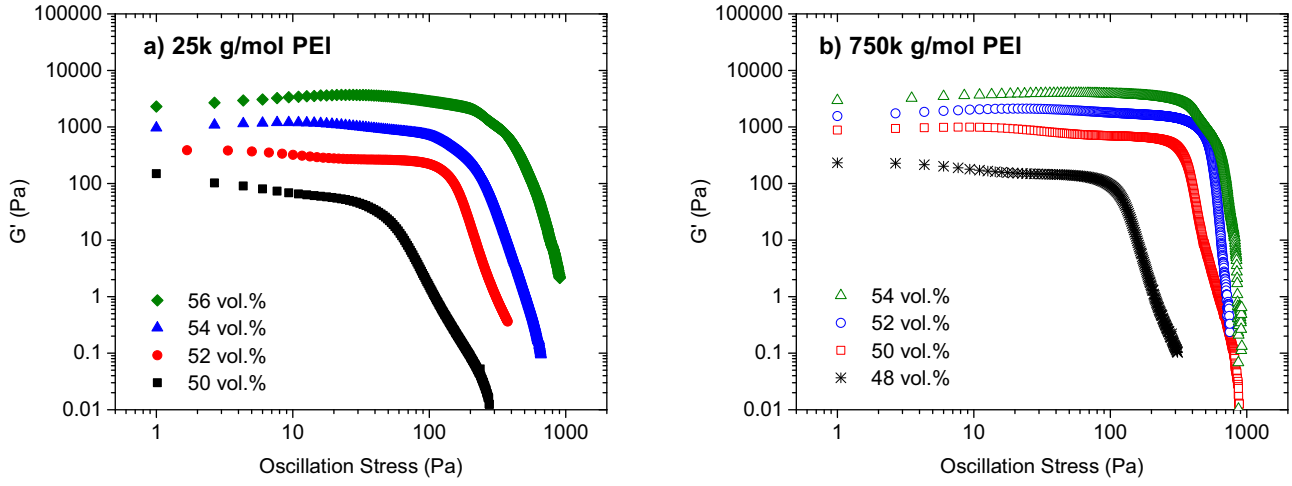

Fig. 4. Log storage modulus (G') vs log oscillation stress plots obtained at a frequency of 1 Hz of varying B_4C suspensions with (a) 25k g/mol PEI and (b) 750k g/mol PEI molecular weight. Increasing the B_4C solid loading and polymer molecular weight resulted in an increase in gel strength (G'_{eq}).

inks/suspensions with higher G'_{eq} or gel strength facilitate stronger shape retention for the deposited layers [16].

3.2. Boron carbide specimens

This study aims to assess the final quality of formed specimens based on filament layer shape retention and warpage upon drying. Specimen shape retention was quantified by measuring the average filament layer height in cross sectional images of green body specimens shown in Fig. 5. The degree of warpage was taken to be the measurement from a flat surface to the bottom of the B_4C specimen at the maximum point of displacement, as shown in Fig. 6. The inset in Fig. 6 shows an aerial view of each specimen. The summaries of measurements for average filament layer height and warpage displacement (X) are shown in Table 1.

The specimen shape retention was found to directly correlate with the suspension yield stress and equilibrium storage modulus. A study on the development of three dimensional periodic structures made with lead zirconate titanate (PZT) colloidal gels found that suspensions with higher yield stresses and gel strengths possess higher shape retention, higher strengths to support additional layers, and decreasing deflection in spanning elements [17].

The supensions made with 50 and 52 vol.% B_4C with 25k g/mol PEI and the 48 vol.% B_4C with 750k g/mol PEI had yield stresses of less than 37 Pa, the lowest viscosity values over the applied shear rates, and G'_{eq} values less than 300 Pa. These suspensions had low shape retention and did not possess sufficient strength to support additonal deposited layers, resulting in filament layers that compressed under the weight of additional layers. It is hard to differentiate between individual filament layers in Fig. 5 for specimens produced with these suspensions. All other suspensions had yield stresses $\geq$43 Pa and equilibrium storage modulus $\geq$700 Pa, which permitted layers with higher shape retention and sufficient strength to support the stacking of additional layers. The 56 vol.% B_4C suspension with 25k g/mol PEI had the highest yield stress and equilibrium storage modulus. Producing components with the highest average layer height (0.85 mm) resulting in a suspension with the highest filament layer shape retention. In general, suspensions made with PEI 750k g/mol molecular weight possessed higher shape retention than suspensions made with PEI 25k g/mol molecular weight for the same solids loading. These observations are in agreement with the rheological data showing that higher molecular weight PEI suspensions have higher yield stresses and equilibrium storage modulus.

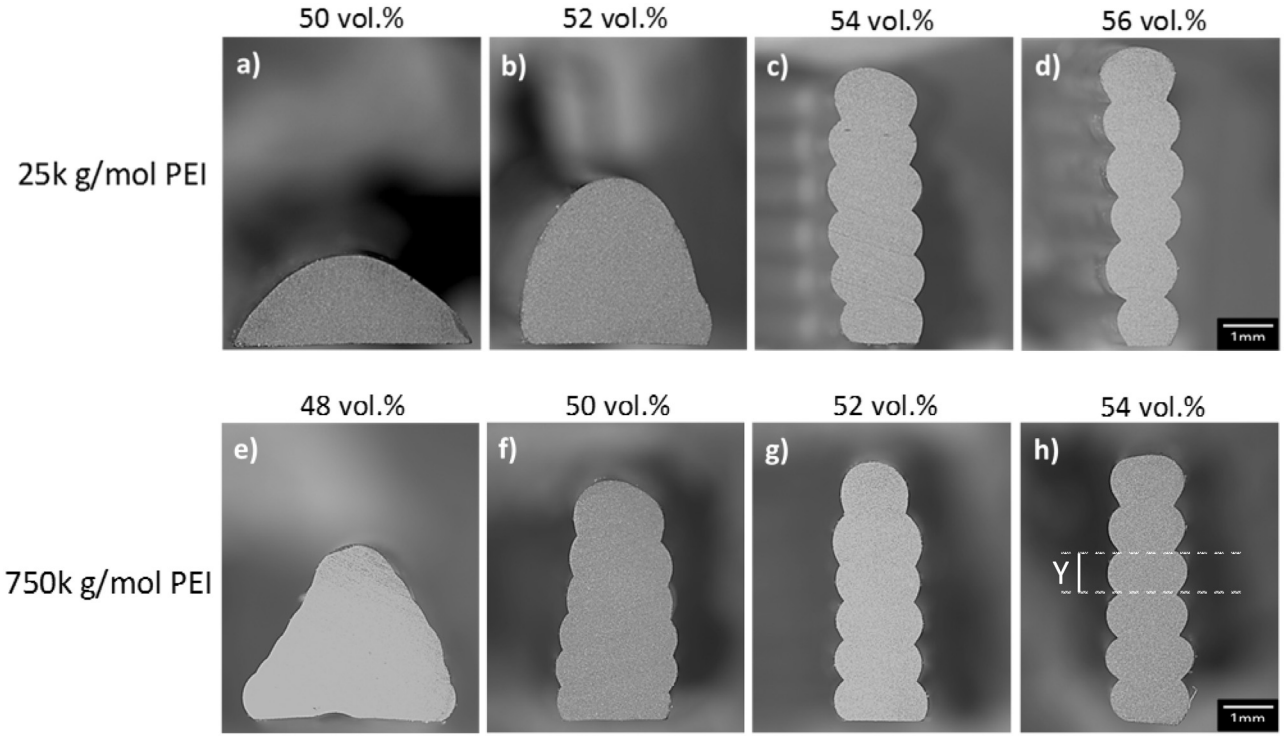

Fig. 5. Cross sectional comparison of green body specimen filament layer heights formed via direct ink writing with varied polymer molecular weight and B_4C solids loading. The measurement of the filament layer height (Y) is illustrated in figure (h) with an average for each specimen shown in Table 1.

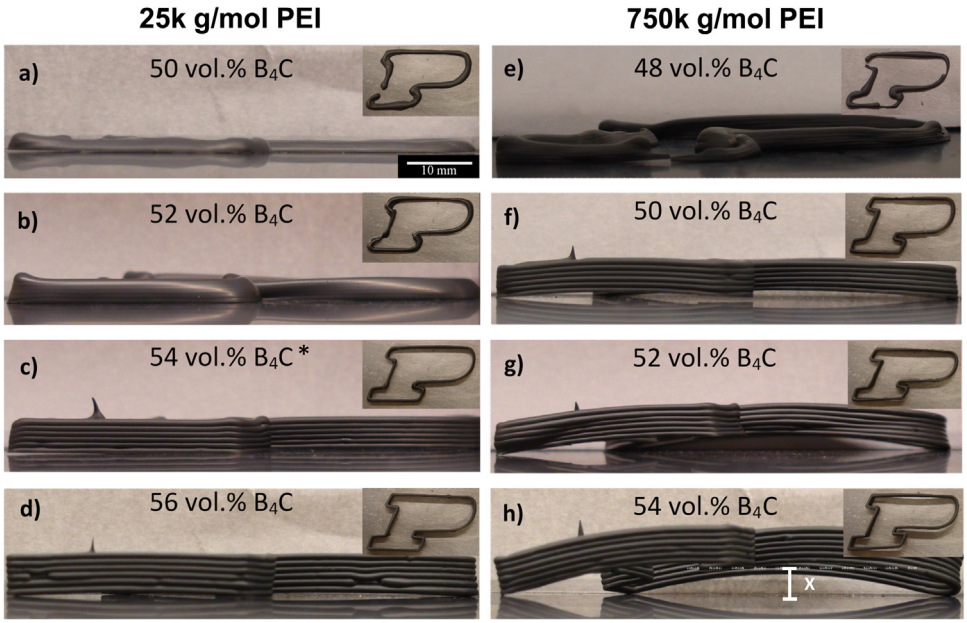

Fig. 6. Profile comparison of samples formed via direct ink writing with varied polymer molecular weight and B_4C solids loading. The inset figure shows the top views of the Purdue "P" and the scale for this image is 5 times smaller than the profile image. Warpage displacement (X) is the measurement from a flat surface to the bottom of the B_4C structure at the maximum point of displacement and is illustrated in image (h).

During the drying process, shrinkage induced warpage effects reduced the final specimen quality. The amount of warpage of each specimen can be seen in the profile images shown in Fig. 6, with warpage displacement values for each shown in Table 1. It was found that an increase in molecular weight of PEI led to an increase in the amount of warpage for suspensions that had sufficient strength to retain a filament shape. This is true for suspensions made with PEI 25k g/mol molecular weight that had a solids loading greater than 54 vol.% and for suspensions made with PEI 750k g/mol molecular weight that had a solids loading of 50 vol.% and greater. This effect could be due to entropic relaxation of the polymer during drying that causes the final specimen to warp. Higher molecular weight polymer melts have been shown to experience more elongation upon extrusion from a capillary that causes them to experience a greater relaxation effect [35]. Narrow molecular weight distributions have also been shown to reduce

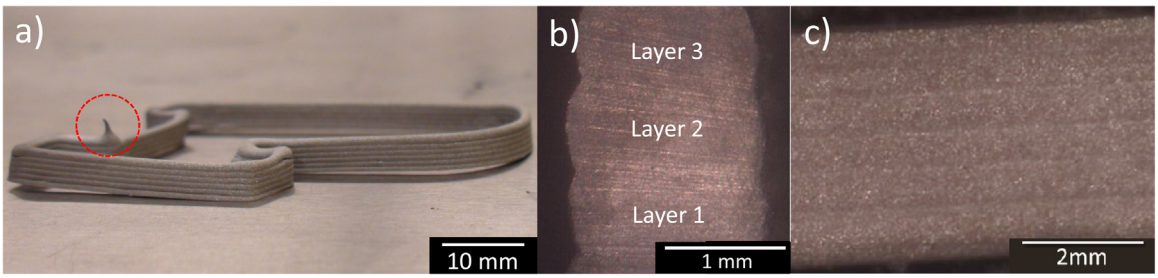

Fig. 7. (a) Sintered sample formed via direct writing a suspension with 54 vol.% B_4C and 25k g/mol PEI. A dashed circle indicates the starting and stopping point for each layer. (b) A cross sectional and (c) profile view of the sintered piece show adhesion between each printed layer.

relaxation effects in polymers [35]. The 750k g/mol and 25k g/mol PEI solutions have a manufacture specified polydispersity index (PDI) of 12.5 and 2.5, respectively. Therefore, the higher PDI of the 750 k g/mol PEI could also be contributing to the larger warpage effects. Increasing solids loading also showed an increase in the amount of specimen warpage for the set of suspensions that had sufficient strength to retain shape. As the solids loading increased, there was a decrease in solvent volume, which has been shown in general polymer systems to lead to a more constrained polymer system with a higher driving force for relaxation [35].

It was determined that the 54 vol.% B_4C suspension with a PEI molecular weight of 25k g/mol produced the highest final quality specimens. Specimens produced with this suspension showed no green body warpage displacement and had adequate strength to retain shape due to its yield stress of 122 Pa and elastic storage modulus of 962 Pa. A final sintered sample formed with this suspension is shown in Fig. 7a, with a cross sectional and profile view shown in Fig. 7b and c, respectively. The cross sectional and profile views of the sintered specimen show adhesion between each printed layer with no systematic residual porosity associated with the forming process for this particular suspension. Comparing the green body specimen image in Fig. 1b and the sintered specimen image in Fig. 7a reveals that there is some final warpage after the sintering process. The warpage could be due to anisotropic shrinkage during sintering and will be examined in further sintering studies.

3.3. Microstructure and density

An SEM micrograph of a sintered and polished specimen made of the optimum suspension of 54 vol.% B_4C with 25k g/mol PEI is shown in Fig. 8. This image is taken from an area between two successive deposited layers and shows no porosity or cracking between layers. There is minimal macroscopic porosity due to forming and a large volume of microscopic porosity seen in the microstructure is due to incomplete sintering.

Chemical analysis of sintered specimens determined that 0.33 wt.% oxygen remained. The minimal oxygen content suggests that the binder burnout and pressureless sintering procedure effectively inhibited the formation of additional oxides in the final specimens due to aqueous processing. Note that the focus of this study was forming, and as such, no sintering aids were added to the suspensions to increase the sintered density. The average density of four sintered specimens made from the optimized suspension was 82% TD, as obtained through Archimedes testing (ASTM 37314) [31]. The true density of the sample is 2.88 g/cm^3 which accounts for the 14.79wt.% W in the sample as determined by ICP-OES outlined in Section 2.3. High densities were not expected due to the relatively low sintering temperature of 2000 °C. Studies using WC as a sintering aid for B_4C found that high densities are only achievable when utilizing liquid phase sintering at temperatures above the WC-B_4C quasibinary eutectic temperature of 2220 °C [26,39]. Below this temperature the WC acts as a solid phase sintering aid that contributes to densification via the addition of a free carbon source, with densities less than 82% TD obtained in previous research when sintering below the eutectic temperature [26,39]. Increasing the sintering temperature through modifications to the current furnace, as well as investigating alternative sintering aids, will be explored as methods to achieve higher density specimens in future studies.

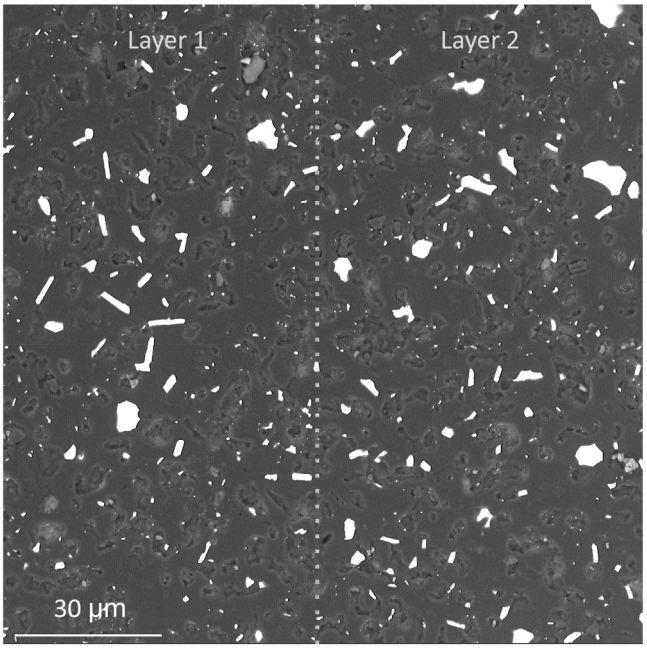

Fig. 8. A representative microstructure taken between two deposited layers of a 54 vol.% B_4C suspension sintered to ~82% TD. Light particles in the image are WC, and porosity is observed from incomplete sintering. A dotted line indicates the interface between two successive layers. No large-scale porosity from forming or cracking between layers is observed.

4. Summary and conclusions

An additive manufacturing technique termed direct ink writing was used to produce near-net shaped B_4C components. The effects of dispersant polymer molecular weight and B_4C solids loading on the rheological properties and final quality of specimens were explored. An increase in the molecular weight of the polymer dispersant (PEI) led to an increase in the yield stress, viscosity, storage shear modulus, and final specimen layer shape retention and warpage. An increase in the yield stress, viscosity, and storage shear modulus of the suspensions correlated to increased layer shape retention and the ability to support additional layers. However, increasing the solids loading decreased the quality of the final specimens due to warpage effects. It was determined that the 54 vol.% B_4C suspension with a PEI molecular weight of 25k g/mol was opti-

mum for direct writing because of the high filament layer shape retention and zero warpage displacement during drying.

Acknowledgements

This work was supported by the U.S. Army Research Office (W911NF-13-0425) with an Undergraduate Research Apprenticeship Program (URAP) supplement. The authors would like to thank Professor Carlos Martinez at Purdue University for his training and for providing the necessary rheometry equipment to perform this study. Also, the authors would like to thank Alycia McEachen and Ross Piedmonte for their help with data collection.

References

[1] P. Dünner, H.-J. Heuvel, M. Hörle, Absorber materials for control rod systems of fast breeder reactors, J. Nucl. Mater. 124 (1984) 185–194.
[2] F. Thévenot, Boron carbide—a comprehensive review, J. Eur. Ceram. Soc. 6 (1990) 205–225.
[3] W.G. Fahrenholtz, E.W. Neuman, H.J. Brown-Shaklee, G.E. Hilmas, Superhard Boride–Carbide particulate composites, J. Am. Ceram. Soc. 93 (2010) 3580–3583.
[4] M.W. Chen, J.W. McCauley, J.C. LaSalvia, K.J. Hemker, Microstructural characterization of commercial hot-pressed boron carbide ceramics, J. Am. Ceram. Soc. 88 (2005) 1935–1942.
[5] A.D. Osipov, I.T. Ostapenko, V.V. Slezov, R.V. Tarasov, V.P. Podtykan, N.F. Kartsev, Effect of porosity and grain size on the mechanical properties of hot-pressed boron carbide, Sov. Powder Metall. Met. Ceram. 21 (1982) 55–58.
[6] S. Leo, C. Tallon, G.V. Franks, Aqueous and nonaqueous colloidal processing of difficult-to-densify ceramics: suspension rheology and particle packing, J. Am. Ceram. Soc. 97 (2014) 3807–3817.
[7] Z. Luo, Z. Lv, D. Jiang, J. Zhang, Z. Chen, Z. Huang, Aqueous tape casting of boron carbide ceramic, Ceram. Int. 39 (2013) 2123–2126.
[8] T.K. Roy, C. Subramanian, A.K. Suri, Pressureless sintering of boron carbide, Ceram. Int. 32 (2006) 227–233.
[9] V.L. Wiesner, Fabricating Complex-Shaped Components by Room-Temperature Injection Molding of Aqueous Ceramic Suspension Gels, Purdue University, 2013.
[10] X. Li, D. Jiang, J. Zhang, Q. Lin, Z. Chen, Z. Huang, The dispersion of boron carbide powder in aqueous media, J. Eur. Ceram. Soc. 33 (2013) 1655–1663.
[11] B. Susmita, V. Sahar, K. Dongxu, A. Bandyopadhyay, Additive manufacturing of ceramics, in: Addit. Manuf., CRC Press, 2015, pp. 143–184.
[12] J.N. Stuecker, J. Cesarano, D.A. Hirschfeld, Control of the viscous behavior of highly concentrated mullite suspensions for robocasting, J. Mater. Process. Technol. 142 (2003) 318–325.
[13] B.H. King, S.L. Morissette, H. Denham, J. Cesarano, D. Dimos, Influence of rheology on deposition behavior of ceramic pastes in direct fabrication systems, Solid Free. Fabr. Proc. (August) (1998) 391–398.
[14] J.A. Lewis, G.M. Gratson, Direct writing in three dimensions, Mater. Today 7 (2004) 32–39.
[15] J. Cesarano, A review of robocasting technology, MRS Proc. 542 (1998).
[16] J.A. Lewis, J.E. Smay, J. Stuecker, J. Cesarano, Direct ink writing of three-dimensional ceramic structures, J. Am. Ceram. Soc. 89 (2006) 3599–3609.
[17] J.E. Smay, J. Cesarano, J.A. Lewis, Colloidal inks for directed assembly of 3-D periodic structures, Langmuir 18 (2002) 5429–5437.
[18] M. Acosta, V.L. Wiesner, C.J. Martinez, R.W. Trice, J.P. Youngblood, Effect of polyvinylpyrrolidone additions on the rheology of aqueous, highly loaded alumina suspensions, J. Am. Ceram. Soc. 96 (2013) 1372–1382.
[19] L.M. Rueschhoff, W.J. Costakis, M.J. Michie, J.P. Youngblood, R.W. Trice, Additive manufacturing of dense ceramic parts via direct ink writing of aqueous alumina suspensions, Int. J. Appl. Ceram. Technol. (2016) (in press).
[20] J. Cesarano, I.A. Aksay, Processing of highly concentrated aqueous alpha-alumina suspensions stabilized with polyelectrolytes, J. Am. Ceram. Soc. 71 (1988) 1062–1067.
[21] A. MATSUMOTO, T. GOTO, A. KAWAKAMI, Slip casting and pressureless sintering of boron carbide and its application to the nuclear field, J. Ceram. Soc. Jpn. 112 (Suppl) (2004) S399–S402, http://dx.doi.org/10.14852/jcersjsuppl.112.0.S399.0.
[22] P.D. Williams, D.D. Hawn, Aqueous dispersion and slip casting of boron carbide powder: effect of pH and oxygen content, J. Am. Ceram. Soc. 74 (1991) 1614–1618.
[23] J. Sun, L. Gao, Dispersing SiC powder and improving its rheological behaviour, J. Eur. Ceram. Soc. 21 (2001) 2447–2451.
[24] A.I. Diaz-Cano, R.W. Trice, J.P. Youngblood, Stabilization and optimization of highly loaded boron carbide suspensions gels., (2016). (unpublished work).
[25] W.B. Russel, D.A. Saville, W.R. Schowalter, Colloidal Dispersions, Cambridge University Press, 1989.
[26] Z. Zakhariev, D. Radev, Dense material obtained on the basis of boron carbide sintered without pressing, in: Adv. Hard Mater. Prod., London, UK, 1988: pp. 3. 1–33.7.
[27] S.-J.L. Kang, Sintering: Densification Grain Growth, and Microstructure, Butterworth-Heinemann, 2005.
[28] V.L. Wiesner, L.M. Rueschhoff, A.I. Diaz-Cano, R.W. Trice, J.P. Youngblood, Producing dense zirconium diboride components by room-temperature injection molding of aqueous ceramic suspensions, Ceram. Int. 42 (2016) 2750–2760.
[29] W.H. Herschel, R. Bulkley, Measurement of consistency as applied to rubber-benzene solutions, Proc. ASTM 26 (Part II) (1926) 621–629.
[30] T.F. Tadros, Rheology of Dispersions: Principles and Applications, John Wiley & Sons, 2010.
[31] Standard Test Method for Water Absorption, Bulk Density, Apparent Porosity, and Apparent Specific Gravity of Fired Whiteware Products, ASTM C373-14a. 88 (2014) 1–2.
[32] H.B. Denham, J. Cesarano, B.H. King, P. Calvert, Mechanical behavior of robocast alumina, Solid Free. Fabr. Proc. (August) (1998) 589–596.
[33] M. Subbanna, S. Malghan, Shear yield stress of flocculated alumina–zirconia mixed suspensions, Chem. Eng. Sci. 53 (1998) 3073–3079.
[34] N.G. McCrum, C.P. Buckley, C.B. Bucknall, Principles of Polymer Engineering, 2nd ed., Oxford University Press, 1997.
[35] Z. Tadmor, C.G. Gogos, Principles of Polymer Processing, second ed., Chemical Pub., New York, 1980.
[36] V.M.B. Moloney, D. Parris, M.J. Edirisinghe, Rheology of zirconia suspensions in a nonpolar organic medium, J. Am. Ceram. Soc. 78 (1995) 3225–3232.
[37] S. Liu, J.H. Masliyah, Suspensions: fundamentals and applications in the petroleum industry, Rheol. Suspens. 2009 (2016) 107–176.
[38] G.M. Channell, C.F. Zukoski, Shear and compressive rheology of aggregated alumina suspensions, AIChE J. 43 (1997) 1700–1708.
[39] L. Sigl, H. Thaler, K.-A. Schwetz, Process for producing bodies based on boron carbide by pressureless sintering, US5505899 A; US 08/260,895; 1996.